

Reconstructing Hand-Held Objects in 3D

Jane Wu¹ Georgios Pavlakos² Georgia Gkioxari³ Jitendra Malik¹

¹ UC Berkeley ² UT Austin ³ Caltech

Abstract. Objects manipulated by the hand (*i.e.*, manipulanda) are particularly challenging to reconstruct from in-the-wild RGB images or videos. Not only does the hand occlude much of the object, but also the object is often only visible in a small number of image pixels. At the same time, two strong anchors emerge in this setting: (1) estimated 3D hands help disambiguate the location and scale of the object, and (2) the set of manipulanda is small relative to all possible objects. With these insights in mind, we present a scalable paradigm for hand-held object reconstruction that builds on recent breakthroughs in large language/vision models and 3D object datasets. Our model, MCC-Hand-Object (MCC-HO), jointly reconstructs hand and object geometry given a single RGB image and inferred 3D hand as inputs. Subsequently, we use GPT-4(V) to retrieve a 3D object model that matches the object in the image and rigidly align the model to the network-inferred geometry; we call this alignment Retrieval-Augmented Reconstruction (RAR). Experiments demonstrate that MCC-HO achieves state-of-the-art performance on lab and Internet datasets, and we show how RAR can be used to automatically obtain 3D labels for in-the-wild images of hand-object interactions.

1 Introduction

“Man is the measure of all things.”

Protagoras

In manipulation, one may philosophize that the *hand* is the measure of all objects. From infancy, humans use their hands to gather information about the physical world [30, 64, 67, 83]. Through our hands and eyes, we learn to estimate 3D geometry and physical properties as well as affordances that inform the ways in which we manipulate objects [14, 39].

Recovering hand-object interactions in 3D is an important problem in both computer vision and robotics. While there has been significant progress in reconstructing hands [50, 52, 63] and objects [36, 37, 85] separately, joint reconstruction of hand-object interactions presents unique challenges that cannot currently be solved by general reconstruction approaches. Procedural methods such as Structure from Motion (SfM) [72] will struggle because the object is mostly occluded, and thus it is difficult to obtain enough feature points to achieve accurate reconstruction. Similarly, Neural Radiance Fields (NeRFs) [44] are best suited for



Fig. 1: We present a scalable approach to hand-held object reconstruction that is guided by recognition and retrieval. In the first stage, our transformer-based model (MCC-HO) infers hand-object 3D geometry from a single RGB image (Row 2, visualized as meshes). In the second stage, a template object model is obtained using Retrieval-Augmented Reconstruction (RAR). This template model is then rigidly aligned with the output of MCC-HO using ICP (Row 3).

unoccluded multiview reconstruction of static scenes and objects. Instead, state-of-the-art approaches in hand-object reconstruction have relied on human assistance for data collection [3, 13, 51]. While manually-retrieved 3D object models naturally improve reconstruction quality and can provide better initialization, this paradigm is not scalable. This is because human-driven retrieval typically includes searching online for a suitable object model, verifying that the model matches the object in the image, and providing an estimate of 3D object pose [3]. Rigidly aligning the 3D model to an image is also an underconstrained 3D-to-2D problem, and optimization approaches are prone to issues with local minima.

In this paper, we present a novel approach to reconstructing hands manipulating common objects from monocular RGB image(s) or video. We draw from three key insights:

1. One can recover shape even from single images at test time, if the object being seen has some family resemblance to previously seen 3D objects. For children, the ability to see 3D from motion comes first, followed by binocular stereopsis, and then finally they can guess 3D shape even from a single image [92]. An operationalization of this in computer vision is the MCC system [85] — the model requires 3D information at training time, but at test time a single image is enough.
2. In images of hand-held objects, we expect to see hands. The hands also provide a strong anchor for 3D location and scale; for instance, the hands provide a convenient measurement tool for many commonplace activities (*e.g.*, cooking, crafts). Recent progress in single-image hand reconstruction [52] enables the development of a robust hand-centric approach to object reconstruction.

- Multiple datasets have now been collected which have videos of hand-object interactions with underlying 3D ground truth (see Section 2), but there has not been a model trained on all available data.

Given an RGB image and estimated 3D hand, we train a transformer-based model, MCC-Hand-Object (MCC-HO), that jointly infers 3D hand and object geometry. This geometry is represented as a neural implicit surface composed of occupancy, color, and hand-object segmentation. Our model architecture is adapted from an existing object reconstruction model, MCC [85], and thus we make use of a learned object prior by fine-tuning an MCC model that is trained on the CO3Dv2 dataset [59].

In conjunction with MCC-HO, we propose Retrieval-Augmented Reconstruction (RAR), a method for automatically retrieving object models using large language/vision models to improve network-inferred geometry. Specifically, we prompt GPT-4(V) [48] to recognize the hand-held object in the image and provide a detailed text description. This description is passed to Genie [42], a text-to-3D generative model, to obtain a 3D object. After the object is retrieved, iterative closest point (ICP) [1] or other point cloud fitting techniques can be used to rigidly align the Genie mesh with the estimated geometry from our network. See Figure 1.

To summarize, this paper presents a paradigm for reconstructing hand-held objects that combines the respective advantages of model-free and model-based approaches. Our method consists of three stages: (1) learning-based hand-object reconstruction, (2) object model retrieval, and (3) rigid alignment of the retrieved model with network-inferred geometry. In the first stage, MCC-HO jointly estimates hand and object geometry from a single RGB image and 3D hand. In the second stage, RAR is used to improve reconstruction quality via recognition and retrieval. The hand-held object is recognized by GPT-4(V) and a 3D object is retrieved using a text-to-3D generative model (*e.g.*, Genie [42]). In the third stage, the retrieved 3D object is rigidly aligned with the network-inferred object geometry. Experiments show that our model outperforms existing methods for hand-held object reconstruction on available datasets containing 3D labels, including DexYCB, MOW, and HOI4D [3, 5, 38]. To demonstrate the scalability of our approach, we additionally use RAR to obtain ground truth 3D hands and objects for previously unlabeled images in the 100DOH dataset [66].

2 Related Work

Object reconstruction. Reconstructing objects from images is a longstanding problem in computer vision, and the bulk of research in this area has focused on scenarios where the object is fully or almost fully unoccluded in the input view(s). Structure from motion (SfM) [21, 65, 68, 72] and SLAM [4, 47, 69] remain robust solutions particularly for multiview reconstruction and camera parameter estimation. Learning-based object reconstruction methods typically represent 3D geometry as point clouds [54, 55], meshes [16, 81, 84], voxel grids [78, 86], or implicit surfaces [44, 46, 49, 71, 79, 85]. Following the release of Objaverse [11]

and Objaverse-XL [10], a number of works have used this large-scale 3D object dataset to train monocular object reconstruction models [26, 36, 37, 40]. The CO3Dv2 dataset [60] contains objects from 50 MS-COCO categories [35] and has also been used to train monocular object reconstruction models [85]. In practice, we find that off-the-shelf object reconstruction methods do not perform well on images of hand-object interactions due to occlusion from the hand, larger object pose diversity, etc.

Hand reconstruction. Recently, there has been a growing body of literature on estimating hand pose from a monocular RGB image [34, 43, 45, 50, 52, 63, 76, 93, 96] or monocular video [28, 82, 88]. These approaches either estimate skeletal joint locations of the hands or use parametric models such as MANO [62]. Since humans have two hands, other methods aim to reconstruct the left and right hands jointly [77, 94]. Particularly relevant to our work, [61] considers the challenging case of predicting pose when the hand is interacting with objects, which can lead to large occlusions of the hand and/or object.

Model-based hand-object pose estimation. When 3D object models are available, the problem of recovering hand-object interactions can be reduced to estimating the pose and shape of the hand and the rigid pose of the object [2, 3, 13, 22, 23, 51, 56, 70, 73, 74, 87, 89]. The estimated hands can then be used to rigidly align the object with images or videos [3, 51] via inverse rendering [41, 58]. However, image-based optimization losses are prone to issues with local minima, as depth/3D information is ambiguous from a single RGB image.

Model-free hand-object reconstruction. Reconstructing hand-held objects without corresponding 3D models poses additional challenges compared to general object reconstruction due to frequent occlusions by the hand and significantly less publicly available 3D data of hand-object interactions. Existing approaches are either tailored to reconstruction from a single image [6–8, 15, 24, 90, 95], RGB video [19, 27, 53, 91], or RGB-D video [80]. Our approach combines the respective benefits of model-based and model-free reconstruction; we first reconstruct 3D objects from a single image, and the output is used to guide the registration of a retrieved template 3D model.

Hand-object datasets. Datasets containing hand-object interactions are either collected in lab environments [2, 5, 20, 31, 38], through large-scale capture [17, 18], or from Internet videos [3, 9, 66]. A number of hand-held object reconstruction models [6–8] were trained on either the HO-3D [20] or DexYCB [5] datasets. Since the combined number of object instances in these two datasets is 31, it is difficult for such approaches to generalize to unseen objects. HOI4D [38] is currently the largest available dataset with 3D hand and object labels (also used in [91]). There is also a comparably larger amount of data containing videos of hand-object interactions without 3D labels. Epic Kitchens [9] contains 55 hours of egocentric video of people in their personal kitchens. Ego4D [17] and Ego-Exo4D [18] are also egocentric datasets, and 100 Days of Hands (100DOH) [66] contains 131 days of footage collected from Internet videos. Following the release of [66], MOW [3] and RHOV [51] labeled a subset of images and video clips from 100DOH, respectively, with 3D hands and objects.

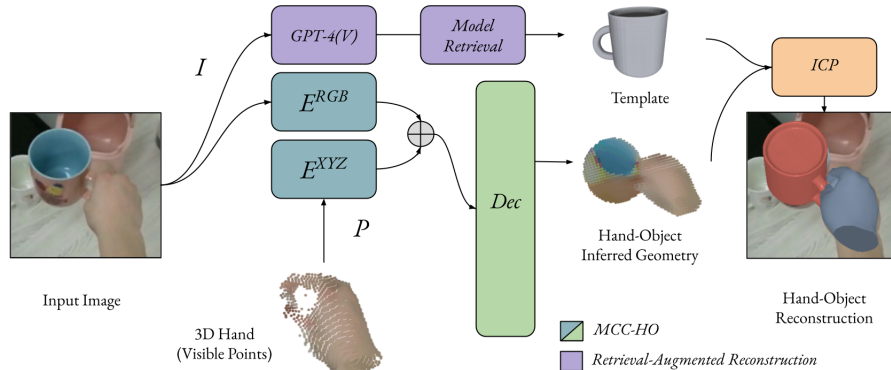


Fig. 2: Given an RGB image and estimated 3D hand, our method reconstructs hand-held objects in three stages. In the first stage, MCC-HO is used to predict hand and object point clouds. In the second stage, a template mesh for the object is obtained using Retrieval-Augmented Reconstruction (RAR). In the third stage, the template object mesh is rigidly aligned to the network-inferred geometry using ICP.

3 Method Overview

We propose a three-stage approach to reconstructing hand-object interactions that combines feedforward network inference with object model retrieval and subsequent 3D fitting. See Figure 2. Our approach is built on two important insights in the hand-object interaction setting. The presence of a human hand provides grounding in terms of both the 3D location and scale of the object. While monocular hand reconstruction is an ill-posed problem and can be a limiting factor for hand-conditioned object reconstruction approaches, recent progress has enabled accurate hand estimation by scaling up [52]. Thus, as in prior work [8,90], the estimated object pose and shape is conditioned on the estimated 3D hand. Applying a hand-centric approach has several advantages. Since monocular image/video reconstruction is particularly ill-posed with respect to depth and scale, 3D hands can be used to disambiguate the location and size of the object. Furthermore, the location of the 3D hand provides a coordinate system for estimating object geometry; in the case of rotating, symmetric objects, the hand can disambiguate the pose of the object.

In addition, although the hand introduces significant occlusions of the object, the space of possible manipulanda is much smaller than the space of all objects. Thus, this work focuses on reconstructing categories of common household objects, similar in spirit to how the COCO dataset [35] was constructed and in alignment with object [60] and hand-object [38] datasets. The pervasiveness of such commonplace objects enables deploying large image recognition systems for the task of automatically recognizing the object and retrieving a 3D object model. Since household manipulanda are often quite uniform in shape (*e.g.*, a knife, an 8 o.z. mug), the accuracy of such a retrieval process is much higher

than for generic objects, whether through lookup in an object dataset [10,11] or text-to-3D generation methods [42] trained on such data.

4 Hand-Object Geometry Inference

In the first stage, hand and object geometry are jointly inferred by training a model adapted from MCC [85] for the specific task of hand-object reconstruction. Notably, two domain shifts from the original MCC model are applied. First, the input depth image is removed and the input RGB-D point cloud is replaced with the 3D hand. Second, the model is trained to infer both hand and object geometry, and thus an extra segmentation output is added to the decoder. We call our model MCC-Hand-Object (MCC-HO).

The inputs to MCC-HO are a single RGB image and 3D hand geometry. Hand and object segmentation masks can be obtained either from ground truth labels or Segment Anything (SAM) [29], and the combined hand-object mask determines the bounding box that is used to crop/resize the input image. Hand geometry is typically parameterized by the MANO hand model [62], which is composed of pose parameters $\theta \in \mathbb{R}^{48}$ and shape parameters $\beta \in \mathbb{R}^{10}$. The MANO hand skeleton contains 21 joints. At training time, the ground truth 3D hand is used. At test time, HaMeR [52] or any other 3D hand estimation methods can be used.

The inferred geometry is represented as a neural implicit function $\rho(x)$ modeling the hand and object jointly, such that for any 3D location x , ρ returns the occupancy probability $\sigma(x)$, RGB color $c(x)$, and segmentation label $m(x)$:

$$\rho(x) = (\sigma(x), c(x), m(x)) \quad (1)$$

where $\sigma(x) \in [0, 1]$, $c(x) \in [0, 1]^3$, and $m(x) \in \{0, 1, 2\}$ to indicating a background, hand, or object point. The scale of the object geometry is normalized with respect to the input 3D hand.

4.1 Architecture

MCC-HO has an encoder-decoder architecture that is composed of transformers [75] and outputs an implicit representation of hand-object geometry. The input images and 3D hand are passed to the encoder to compute a feature map that is a function of both image and hand embeddings. These features are then used to condition the decoder, which maps any 3D location to occupancy, color, and hand-object segmentation. During training, a set of query 3D points Q are uniformly sampled within the bounds of a normalized volume. At test time, vertices of a voxel grid are passed as query points.

Encoder. The encoder takes as input a single RGB image $I \in \mathbb{R}^{H \times W \times 3}$ and a posed MANO hand mesh defined in camera world space with vertices $v_h \in \mathbb{R}^{778 \times 3}$ and faces $f_h \in \mathbb{R}^{1538 \times 3}$. The camera intrinsics are either known or consistent with the estimated 3D hand (*e.g.*, the camera parameters used during

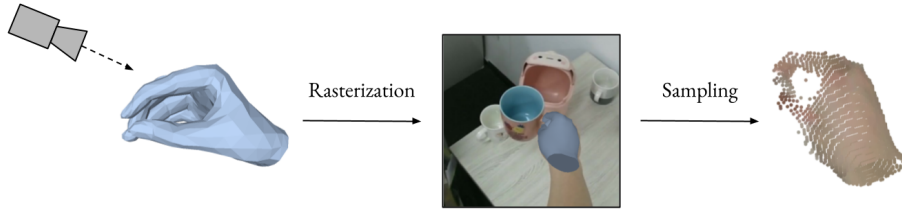


Fig. 3: The input 3D hand is rasterized and per-pixel 3D points are sampled to be passed to the MCC-HO encoder.

HaMeR inference [52]). In order to jointly encode the image and hand geometry, the hand mesh is rasterized and per-pixel 3D points for the hand are sampled. For each pixel (i, j) in the image, a ray is cast from the camera aperture to the pixel center to determine the first intersection point with the hand mesh at a point $P_0(i, j)$ in camera world space. If an intersection exists, the 3D location of each point is barycentrically interpolated from the intersecting camera world space triangle vertices, denoted $\{v_{h,1}, v_{h,2}, v_{h,3}\}$, such that:

$$P_0(i, j) = \alpha_1 v_{h,1} + \alpha_2 v_{h,2} + \alpha_3 v_{h,3} \in \mathbb{R}^3, \quad (2)$$

with barycentric weights α . The points P_0 are used to define a normalized camera world space, such that the 3D coordinates passed to the network are $P = s(P_0 - \mu(P_0))/\sigma(P_0)$ and geometry is inferred in this same coordinate system. Importantly, s is a constant scaling factor used to ensure the object geometry can be contained by the bounds of this hand-normalized sampling space. See Figure 3.

The image I and hand points P are encoded into a single representation R , where:

$$R := f(E^{RGB}(I), E^{XYZ}(P)) \in \mathbb{R}^{N^{enc} \times C}, \quad (3)$$

and E^{RGB} and E^{XYZ} are identical to the transformers proposed in MCC [85], though we define P differently, *i.e.*, without an input depth image. The image transformer E^{RGB} has a Vision Transformer (ViT) architecture [12] with 16×16 patch embeddings. The point transformer E^{XYZ} uses a self-attention-based patch embedding design that differentiates between seen and unseen pixel points. In particular, for points in P where no ray-mesh intersection was found, a special C -dimensional embedding is learned in lieu of embedding 3D points. The function f concatenates the output of the two transformers, each of which has dimensions $N^{enc} \times C$. N^{enc} is the number of tokens used in the transformers and C is the output channel size.

Decoder. The decoder takes as input the encoder output, R , as well as a set of query points $Q \in \mathbb{R}^{N_q \times 3}$ (we choose $N_q = 1024$). These inputs are passed to a transformer with architecture adopted from MCC and inspired by Masked Autoencoders (MAE) [25]. Each query token is passed to three output heads

that infer binary occupancy σ , RGB color c , and hand-object segmentation m , such that:

$$\text{Decoder}(R, Q) := (\sigma(Q), c(Q), m(Q)). \quad (4)$$

The decoder layers that output occupancy and color align with MCC, but MCC-HO has an additional linear layer that infers multiclass segmentation of each point into either background, hand, or object labels.

As discussed in further detail in MCC, a point-query-based decoder presents a number of advantages with respect to computational efficiency and scalability. Since the encoder is independent of the point queries, any number of points can be sampled using the same encoder structure and feature map size. The decoder architecture is relatively lightweight and also enables dynamic changes to the point sampling resolution and query size at training and/or test time.

4.2 Implementation Details

The training loss is a combination of occupancy, color, and segmentation:

$$\mathcal{L} = \mathcal{L}_\sigma + \mathcal{L}_c(\sigma_{gt}) + \mathcal{L}_m \quad (5)$$

The occupancy loss \mathcal{L}_σ is a binary cross-entropy loss comparing the predicted and ground truth occupancies of each query point. The color loss \mathcal{L}_c is a 256-way classification loss computed for query points that have ground truth occupancy of 1. The segmentation loss \mathcal{L}_m is 3-way classification loss for each query point corresponding to background (empty space), hand, and object labels.

Our model was trained on a single Quadro RTX 8000 for 3k epochs with a learning rate of $1e^{-5}$ and batch size of 16. We use a cosine schedule and a linear warm-up for the first 5 epochs. At each epoch, one random frame from each sequence is selected. Network parameters that correspond to the MCC architecture [85] were initialized using a pretrained MCC model that was trained on the CO3Dv2 dataset [60]. The weights of the additional linear layer in our decoder that outputs hand-object segmentation are initialized via Xavier initialization.

5 Retrieval-Augmented Reconstruction

In order to further improve upon the network-inferred object geometry, we use GPT-4(V) [48] to automatically detect and retrieve a 3D object corresponding to the hand-held object in an image. We coin this technique Retrieval-Augmented Reconstruction (RAR) in reference to Retrieval-Augmented Generation in natural language processing [32].

Given an input image (one could also use stacked video frames), we prompt GPT-4(V) to provide a detailed description of the object the hand is holding. This text caption is passed to Genie, a text-to-3D model from Luma [42], to retrieve realistic 3D object geometry and appearance (Genie is also used in [33]). See Figure 4. After the object model is obtained, it is rigidly aligned with our network-inferred object geometry using ICP [1]. In particular, we sample a set

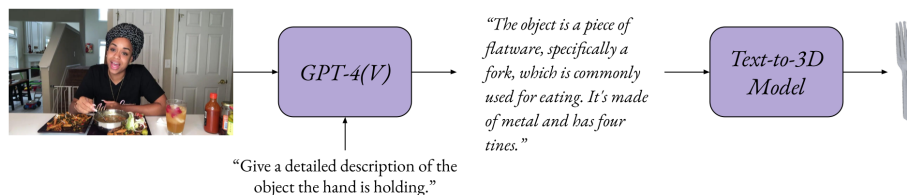


Fig. 4: Retrieval-Augmented Reconstruction (RAR). Given an input image, we prompt GPT-4(V) [48] to recognize and provide a text description of the hand-held object. The text description is passed to a text-to-3D model (in our case, Genie [42]) to obtain a 3D object.

of random initial rotations for the retrieved 3D model and select the ICP transformation that results in the lowest alignment error. Genie outputs geometry normalized with respect to a unit cube, so the scale of the 3D model is initialized using the bounding volume of the predicted object point cloud.

6 Experiments

Section 6.1 details the datasets that were used for training and evaluation. Section 6.2 defines the evaluation metrics used for comparisons. Section 6.3 quantifies the advantages of using MCC-HO, *e.g.*, a hand-centric approach, in comparison to the original MCC model [85]. We also quantitatively (Section 6.4) and qualitatively (Section 6.5) evaluate our model against existing work in model-free, monocular hand-object reconstruction [24, 90] and find that MCC-HO achieves state-of-the-art performance on all three datasets used [3, 5, 38]. In particular, the methods most similar to ours are HO [24] and IHOI [90]. The quality of the MCC-HO predicted geometry is also shown to be sufficient for accurate rigid alignment of template objects using ICP. Also in Section 6.5, we provide qualitative results for our Retrieval-Augmented Reconstruction (RAR) approach on in-the-wild Internet images to demonstrate the feasibility and scalability of our automated model retrieval and fitting. Specifically, we apply MCC-HO and RAR to unlabeled images from the 100DOH dataset [66].

6.1 Datasets

We experiment on four different datasets for hand-object reconstruction.

HOI4D: The HOI4D dataset [38] consists of 4,000 lab videos of hands interacting with specified categories of common objects. We selected all sequences containing one of 6 hand-held object categories, and divide the sequences into training, validation and test sets. In total, we used 1142 training sequences, 6 validation sequences, and 12 test sequences consistent with DiffHOI [91]. For the validation set, we selected one video per category and favored object instances that appear the least frequently in the dataset.

DexYCB: The DexYCB dataset [5] contains 1,000 lab videos of hands interacting with 21 YCB objects. We used the “s0” dataset split, which contains 800 training, 40 validation, and 160 test sequences (consistent with prior work [6, 7]).

MOW/RHOV: MOW [3] is a dataset of 512 images from 100 Days of Hands [66] labeled with 3D hands and objects. We use the same splits as [90] with 350 training images and 92 test images. Additionally, we use 110 videos from RHOV [51], each of which is a 2 second clip centered at the corresponding MOW frame. In the RHOV dataset, 19 videos overlap with the MOW test set and thus we do not use them during training.

100DOH: The 100 Days of Hands dataset [66] contains 131 days of footage collected from Internet videos showing hands interacting with objects. The vast majority of videos do not have associated 3D hand or object labels, so we evaluate how well our approach generalizes using examples from this unlabeled subset.

For DexYCB [5], MOW [3], and HOI4D [38], all results generated using our approach use the ground truth 3D hand provided by each dataset. For 100DOH [66] results (*e.g.*, examples not contained in MOW), we use HaMeR [52] to estimate the 3D hand.

6.2 Evaluation Metrics

Since the focus of our approach is on the object manipulated by the hand, we quantitatively evaluate object reconstruction quality using standard 3D metrics, Chamfer Distance (CD) and F-score reported at 5mm and 10mm. Both metrics are computed on point sets, and thus the point clouds inferred by MCC-HO are directly used. The 3D hand provided by each dataset is used as input; note that MOW uses FrankMocap [63] and HOI4D optimizes hand pose using 2D keypoint annotations. For each example, we sample 10k points on the surface of the ground truth mesh consistent with [90, 91] (no transformations are applied to the ground truth geometry). The MCC-HO predicted point clouds are supersampled/subsampled to obtain 10k points as well. In order to account for unknown ground truth camera parameters, ICP with scaling [58] is used to align all predicted geometry with the ground truth mesh. Median metrics are reported for each test dataset.

Chamfer Distance: The Chamfer Distance metric we use between two point sets $A, B \in \mathbb{R}^{N \times 3}$ is:

$$CD(A, B) = \frac{1}{N} \sum_{a \in A} \min_{b \in B} \|a - b\|_2^2 + \frac{1}{N} \sum_{b \in B} \min_{a \in A} \|a - b\|_2^2, \quad (6)$$

where the point sets should have the same size. This equation is consistent with prior work [6, 7, 90, 91]. We report the Chamfer Distance in cm^2 as in [6, 7].

F-score: For 3D evaluation of predicted points, the F-score at a given threshold t is defined as:

$$F_1(X_{pd}, X_{gt}) = 2 \frac{\text{Precision}(X_{pd}, X_{gt}, t) \cdot \text{Recall}(X_{pd}, X_{gt}, t)}{\text{Precision}(X_{pd}, X_{gt}, t) + \text{Recall}(X_{pd}, X_{gt}, t)}. \quad (7)$$

Model Parameters	F-5 (\uparrow)	F-10 (\uparrow)	CD (\downarrow)
MCC [85]	0.10	0.21	31.6
MCC-HO	0.15	0.31	15.2

Table 1: Analysis of how hand-held object reconstruction benefits from conditioning on the hand. Median Chamfer Distance (cm^2) and F-score (5mm, 10mm) metrics for MCC and MCC-HO are computed on the MOW test dataset.

	DexYCB			MOW			HOI4D		
	F-5 (\uparrow)	F-10 (\uparrow)	CD (\downarrow)	F-5 (\uparrow)	F-10 (\uparrow)	CD (\downarrow)	F-5 (\uparrow)	F-10 (\uparrow)	CD (\downarrow)
HO [24]	0.24	0.48	4.76	0.03	0.06	49.8	0.28	0.51	3.86
IHOI [90]	-	-	-	0.13	0.24	23.1	0.42	0.70	2.7
MCC-HO	0.36	0.60	3.74	0.15	0.31	15.2	0.52	0.78	1.36

Table 2: We compare our method, MCC-HO, to prior works on held-out test images from DexYCB, MOW, and HOI4D. Chamfer Distance (cm^2) and F-score (5mm, 10mm) are reported.

6.3 MCC Baseline

Because our model is built on top of MCC [85], we begin by evaluating whether MCC-HO leads to performance gains for the task of hand-held object reconstruction. For MCC, we use the released model that was trained on the CO3Dv2 dataset [60] and apply an existing monocular depth estimator [57] to obtain depth maps (as MCC takes an RGB-D image as input). Table 1 compares 3D metrics between MCC and MCC-HO computed on the MOW test set. We find that fine-tuning MCC for the specific task of hand-held object reconstruction improves performance on test images unseen by both models.

6.4 Quantitative Evaluation

MCC-HO is quantitatively evaluated on a variety of labeled hand-object datasets and in comparison to existing model-free reconstruction approaches [24, 90]. See Table 2. In order to sample points more densely in hand-object regions, the dimensions and granularity of the voxel grid used to query MCC-HO are determined from an initial coarse prediction using a default voxel grid. For DexYCB, we use every 5th frame of the “s0” test split, and for HOI4D, we use all frames from the 12 test sequences that contain a ground truth 3D hand label. The results for IHOI [90] and HO [24] evaluated on the MOW dataset are obtained from the IHOI and DiffHOI [91] papers. Because AlignSDF [7] and gSDF [6] trained DexYCB-specific models, whereas we train a single model on multiple datasets, we do not compare to their published metrics.

Our method achieves state-of-the-art performance for the Chamfer Distance and F-score metrics on all three datasets, implying that our technique is not



Fig. 5: MCC-HO results for MOW test examples. The input image (top, left), network-inferred hand-object point cloud (top, right), rigid alignment of the ground truth mesh with the point cloud using ICP (bottom, left), and an alternative view of the point cloud (bottom, right) are shown.

overfitted to any particular dataset. We conjecture that increasing the number of unique object instances seen during training is important to model generalization. In addition, the pretrained MCC model provides a strong object prior for initialization.

6.5 Qualitative Evaluation

We qualitatively evaluate (1) the reconstruction quality of MCC-HO and (2) how well template objects can be rigidly aligned to the predicted point clouds in 3D (a necessary and sufficient condition for downstream tasks). Figure 5 shows predicted point clouds for a number of MOW test examples, as well as the result of rigidly aligning the ground truth CAD model with each point cloud using ICP. Since MCC-HO is trained with monocular images, the predicted RGB colors are only valid when viewed from the given camera. Because the object geometry is conditioned on the 3D hand, our approach tends to predict reasonable hand-object contact. Additionally, the object in contact with the hand is correctly identified by MCC-HO despite being provided a hand-object bounding box and no segmentation maps.

Figure 6 shows additional visualizations of applying rigid alignment of the template model to MCC-HO results. We include held-out test examples from all three datasets used for training: MOW, DexYCB, and HOI4D. Because MCC-HO is fine-tuned from a general object reconstruction transformer model (MCC), it is robust to unseen object instances at test time. For instance, objects in the MOW test images were never seen by MCC-HO during training. From a practical standpoint, we find 3D-to-3D fitting of template objects with the MCC-HO predicted geometry (*e.g.*, via ICP) to be significantly more efficient than prior 3D-to-2D or per-example optimization approaches [3, 51, 91]. Moreover, optimizing 3D pose with respect to 2D images tends to get stuck in local minima. As Figure 6 demonstrates, this 3D fitting results in physically plausible hand-object interactions that when projected align with the image data.

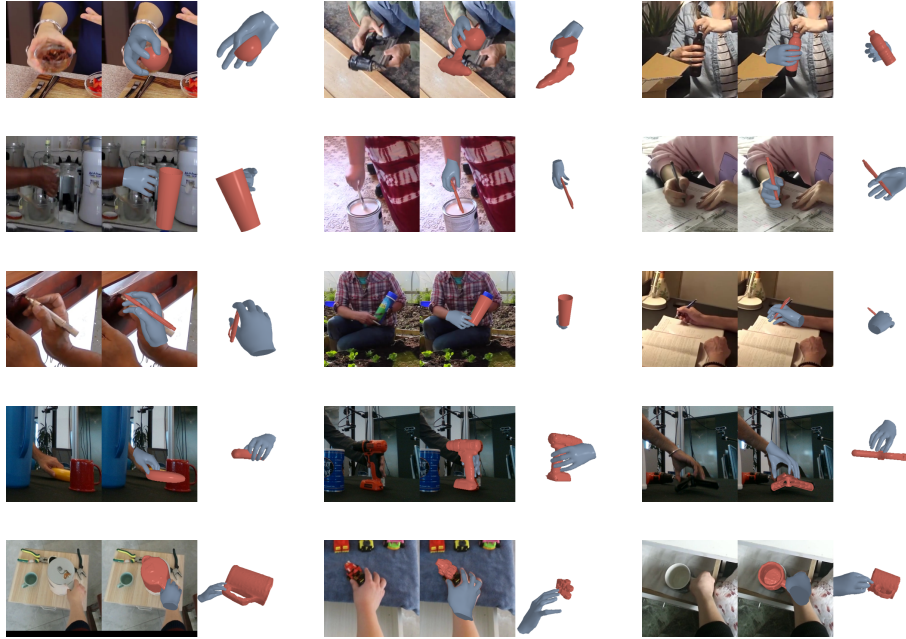


Fig. 6: Our approach applied to test images from MOW (Rows 1-3), DexYCB (Row 4), and HOI4D (Row 5). Each example includes the input image (left), rigid alignment of the ground truth mesh with the MCC-HO predicted point cloud using ICP (middle), and an alternative view (right).

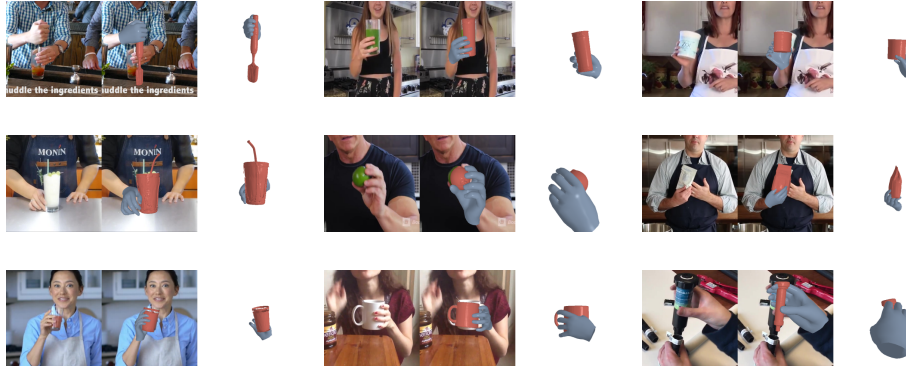


Fig. 7: Our approach applied to images in the 100 Days of Hands dataset [66]. For each image, we estimate 3D hands using HaMeR [52], inference object geometry using MCC-HO, retrieve a 3D model using RAR (*e.g.*, GPT-4(V) and Genie), and rigidly align the 3D model with the inferred point cloud from MCC-HO.

Retrieval-Augmented Reconstruction. The ultimate goal of RAR is to provide a scalable paradigm for creating large hand-object 3D datasets; to this end, we explore the potential to scale up our approach on unlabeled images. Specifically, we take 9 images from 100DOH [66] that do not have 3D ground truth (*e.g.*, not in MOW) and apply MCC-HO combined with RAR to reconstruct hand-object 3D geometry. See Figure 7. Estimated 3D hands for each image are obtained using HaMeR [52]. At test time, our method does not require an input hand-object segmentation mask [3, 51], depth image [85], or hand joint locations [8, 90]. Rather, we simply run feed-forward inference using MCC-HO, retrieve a 3D object mesh using RAR, and run ICP to align this mesh with the inferred point cloud. As more training data is collected through RAR and human-in-the-loop verification, we expect MCC-HO to naturally improve as well (similar in spirit to the data collection process used in Segment Anything [29]).

6.6 Limitations

While our 3D-to-3D rigid alignment approach using ICP is efficient, some misalignment may occur when rendering the reconstruction from the input view camera. This is because we do not use image-based cues for alignment, but note that this can be easily fixed via inverse rendering as in [3, 51]. In particular, the 6DOF object pose can be fine-tuned by minimizing the silhouette loss and hand-object contact/collision losses defined in [3]. See Figure 8. Regardless, our reconstruction provides a more automatic/robust initialization of the 3D object model than manual or random initialization, as was done in prior work [3, 51]. In addition, because MCC-HO is conditioned on an input 3D hand, the accuracy of the predicted hand pose naturally affects object reconstruction performance.



Fig. 8: The input image is not used when running ICP, which can sometimes result in image misalignment errors (Row 1). A postprocess can be applied to resolve silhouette misalignment and any hand-object contact issues (Row 2).

7 Conclusion

In this paper, we present a novel paradigm for reconstructing hand-held objects that combines the respective benefits of model-free and model-based prediction. Our transformer-based model, MCC-HO, is trained to predict hand-object geometry given a single RGB image and estimated 3D hand. Experiments conducted using the DexYCB, MOW, and HOI4D datasets all demonstrate that MCC-HO achieves state-of-the-art performance in hand-held object reconstruction. We additionally present Retrieval-Augmented Reconstruction (RAR), an automatic method for object model retrieval that leverages recent advances in large language/vision models and 3D object datasets. These two approaches can be combined to scale the amount of labeled hand-object interaction data, as suggested by our results using unlabeled 100DOH images [66]. The combination of MCC-HO and RAR can enable the construction of large hand-object datasets at-scale; for future work, we plan to expand on this paradigm to label a larger dataset of Internet videos.

Acknowledgements

We would like to thank Ilija Radosavovic for helpful discussions and feedback. This work was supported by ONR MURI N00014-21-1-2801. J. W. was supported by the NSF Mathematical Sciences Postdoctoral Fellowship and the UC President’s Postdoctoral Fellowship.

References

1. Arun, K.S., Huang, T.S., Blostein, S.D.: Least-squares fitting of two 3-d point sets. *IEEE Transactions on Pattern Analysis and Machine Intelligence* **PAMI-9**(5), 698–700 (1987). <https://doi.org/10.1109/TPAMI.1987.4767965>
2. Bhatnagar, B.L., Xie, X., Petrov, I.A., Sminchisescu, C., Theobalt, C., Pons-Moll, G.: Behave: Dataset and method for tracking human object interactions. In: *Proceedings of the IEEE/CVF Conference on Computer Vision and Pattern Recognition*. pp. 15935–15946 (2022)
3. Cao, Z., Radosavovic, I., Kanazawa, A., Malik, J.: Reconstructing hand-object interactions in the wild. In: *Proceedings of the IEEE/CVF International Conference on Computer Vision*. pp. 12417–12426 (2021)
4. Castellanos, J.A., Montiel, J.M., Neira, J., Tardós, J.D.: The spmap: A probabilistic framework for simultaneous localization and map building. *IEEE Transactions on robotics and Automation* **15**(5), 948–952 (1999)
5. Chao, Y.W., Yang, W., Xiang, Y., Molchanov, P., Handa, A., Tremblay, J., Narang, Y.S., Van Wyk, K., Iqbal, U., Birchfield, S., et al.: Dexycb: A benchmark for capturing hand grasping of objects. In: *Proceedings of the IEEE/CVF Conference on Computer Vision and Pattern Recognition*. pp. 9044–9053 (2021)
6. Chen, Z., Chen, S., Schmid, C., Laptev, I.: gsd: Geometry-driven signed distance functions for 3d hand-object reconstruction. In: *Proceedings of the IEEE/CVF Conference on Computer Vision and Pattern Recognition*. pp. 12890–12900 (2023)

7. Chen, Z., Hasson, Y., Schmid, C., Laptev, I.: Alignsdf: Pose-aligned signed distance fields for hand-object reconstruction. In: European Conference on Computer Vision. pp. 231–248. Springer (2022)
8. Choi, H., Chavan-Daffe, N., Yuan, J., Isler, V., Park, H.: Handnerf: Learning to reconstruct hand-object interaction scene from a single rgb image. arXiv preprint arXiv:2309.07891 (2023)
9. Damen, D., Doughty, H., Farinella, G.M., Fidler, S., Furnari, A., Kazakos, E., Moltisanti, D., Munro, J., Perrett, T., Price, W., et al.: Scaling egocentric vision: The epic-kitchens dataset. In: Proceedings of the European conference on computer vision (ECCV). pp. 720–736 (2018)
10. Deitke, M., Liu, R., Wallingford, M., Ngo, H., Michel, O., Kusupati, A., Fan, A., Laforte, C., Voleti, V., Gadre, S.Y., et al.: Objaverse-xl: A universe of 10m+ 3d objects. Advances in Neural Information Processing Systems **36** (2024)
11. Deitke, M., Schwenk, D., Salvador, J., Weihs, L., Michel, O., VanderBilt, E., Schmidt, L., Ehsani, K., Kembhavi, A., Farhadi, A.: Objaverse: A universe of annotated 3d objects. In: Proceedings of the IEEE/CVF Conference on Computer Vision and Pattern Recognition. pp. 13142–13153 (2023)
12. Dosovitskiy, A., Beyer, L., Kolesnikov, A., Weissenborn, D., Zhai, X., Unterthiner, T., Dehghani, M., Minderer, M., Heigold, G., Gelly, S., et al.: An image is worth 16x16 words: Transformers for image recognition at scale. arXiv preprint arXiv:2010.11929 (2020)
13. Fan, Z., Taheri, O., Tzionas, D., Kocabas, M., Kaufmann, M., Black, M.J., Hilliges, O.: Arctic: A dataset for dexterous bimanual hand-object manipulation. In: Proceedings of the IEEE/CVF Conference on Computer Vision and Pattern Recognition. pp. 12943–12954 (2023)
14. Federico, G., Brandimonte, M.A.: Looking to recognise: the pre-eminence of semantic over sensorimotor processing in human tool use. Scientific reports **10**(1), 6157 (2020)
15. Fu, B., Di, Y., Zhang, C., Wang, G., Huang, Z., Leng, Z., Manhardt, F., Ji, X., Tombari, F.: Hacd: Hand-aware conditional diffusion for monocular hand-held object reconstruction. arXiv preprint arXiv:2311.14189 (2023)
16. Gkioxari, G., Malik, J., Johnson, J.: Mesh r-cnn. In: Proceedings of the IEEE/CVF international conference on computer vision. pp. 9785–9795 (2019)
17. Grauman, K., Westbury, A., Byrne, E., Chavis, Z., Furnari, A., Girdhar, R., Hamburger, J., Jiang, H., Liu, M., Liu, X., et al.: Ego4d: Around the world in 3,000 hours of egocentric video. In: Proceedings of the IEEE/CVF Conference on Computer Vision and Pattern Recognition. pp. 18995–19012 (2022)
18. Grauman, K., Westbury, A., Torresani, L., Kitani, K., Malik, J., Afouras, T., Ashutosh, K., Baiyya, V., Bansal, S., Boote, B., et al.: Ego-exo4d: Understanding skilled human activity from first-and third-person perspectives. arXiv preprint arXiv:2311.18259 (2023)
19. Hampali, S., Hodan, T., Tran, L., Ma, L., Keskin, C., Lepetit, V.: In-hand 3d object scanning from an rgb sequence. In: Proceedings of the IEEE/CVF Conference on Computer Vision and Pattern Recognition. pp. 17079–17088 (2023)
20. Hampali, S., Rad, M., Oberweger, M., Lepetit, V.: Honnotate: A method for 3d annotation of hand and object poses. In: CVPR (2020)
21. Hartley, R., Zisserman, A.: Multiple view geometry in computer vision. Cambridge university press (2003)
22. Hasson, Y., Tekin, B., Bogo, F., Laptev, I., Pollefeys, M., Schmid, C.: Leveraging photometric consistency over time for sparsely supervised hand-object construc-

- tion. In: Proceedings of the IEEE/CVF conference on computer vision and pattern recognition. pp. 571–580 (2020)
23. Hasson, Y., Varol, G., Schmid, C., Laptev, I.: Towards unconstrained joint hand-object reconstruction from rgb videos. In: 2021 International Conference on 3D Vision (3DV). pp. 659–668. IEEE (2021)
 24. Hasson, Y., Varol, G., Tzionas, D., Kalevatykh, I., Black, M.J., Laptev, I., Schmid, C.: Learning joint reconstruction of hands and manipulated objects. In: Proceedings of the IEEE/CVF conference on computer vision and pattern recognition. pp. 11807–11816 (2019)
 25. He, K., Chen, X., Xie, S., Li, Y., Dollár, P., Girshick, R.: Masked autoencoders are scalable vision learners. In: Proceedings of the IEEE/CVF conference on computer vision and pattern recognition. pp. 16000–16009 (2022)
 26. Hong, Y., Zhang, K., Gu, J., Bi, S., Zhou, Y., Liu, D., Liu, F., Sunkavalli, K., Bui, T., Tan, H.: Lrm: Large reconstruction model for single image to 3d. arXiv preprint arXiv:2311.04400 (2023)
 27. Huang, D., Ji, X., He, X., Sun, J., He, T., Shuai, Q., Ouyang, W., Zhou, X.: Reconstructing hand-held objects from monocular video. In: SIGGRAPH Asia 2022 Conference Papers. pp. 1–9 (2022)
 28. Karunratanakul, K., Prokudin, S., Hilliges, O., Tang, S.: Harp: Personalized hand reconstruction from a monocular rgb video. In: Proceedings of the IEEE/CVF Conference on Computer Vision and Pattern Recognition (CVPR). pp. 12802–12813 (June 2023)
 29. Kirillov, A., Mintun, E., Ravi, N., Mao, H., Rolland, C., Gustafson, L., Xiao, T., Whitehead, S., Berg, A.C., Lo, W.Y., et al.: Segment anything. arXiv preprint arXiv:2304.02643 (2023)
 30. Klatzky, R.L., McCloskey, B., Doherty, S., Pellegrino, J., Smith, T.: Knowledge about hand shaping and knowledge about objects. *Journal of motor behavior* **19**(2), 187–213 (1987)
 31. Kwon, T., Tekin, B., Stühmer, J., Bogo, F., Pollefeys, M.: H2o: Two hands manipulating objects for first person interaction recognition. In: Proceedings of the IEEE/CVF International Conference on Computer Vision. pp. 10138–10148 (2021)
 32. Lewis, P., Perez, E., Piktus, A., Petroni, F., Karpukhin, V., Goyal, N., Küttler, H., Lewis, M., Yih, W.t., Rocktäschel, T., et al.: Retrieval-augmented generation for knowledge-intensive nlp tasks. *Advances in Neural Information Processing Systems* **33**, 9459–9474 (2020)
 33. Li, J., Wu, J., Liu, C.K.: Object motion guided human motion synthesis. *ACM Transactions on Graphics (TOG)* **42**(6), 1–11 (2023)
 34. Li, M., An, L., Zhang, H., Wu, L., Chen, F., Yu, T., Liu, Y.: Interacting attention graph for single image two-hand reconstruction. In: Proceedings of the IEEE/CVF Conference on Computer Vision and Pattern Recognition. pp. 2761–2770 (2022)
 35. Lin, T.Y., Maire, M., Belongie, S., Hays, J., Perona, P., Ramanan, D., Dollár, P., Zitnick, C.L.: Microsoft coco: Common objects in context. In: *Computer Vision—ECCV 2014: 13th European Conference, Zurich, Switzerland, September 6–12, 2014, Proceedings, Part V* 13. pp. 740–755. Springer (2014)
 36. Liu, M., Xu, C., Jin, H., Chen, L., Varma T, M., Xu, Z., Su, H.: One-2-3-45: Any single image to 3d mesh in 45 seconds without per-shape optimization. *Advances in Neural Information Processing Systems* **36** (2024)
 37. Liu, R., Wu, R., Van Hoorick, B., Tokmakov, P., Zakharov, S., Vondrick, C.: Zero-1-to-3: Zero-shot one image to 3d object. In: Proceedings of the IEEE/CVF International Conference on Computer Vision. pp. 9298–9309 (2023)

38. Liu, Y., Liu, Y., Jiang, C., Lyu, K., Wan, W., Shen, H., Liang, B., Fu, Z., Wang, H., Yi, L.: Hoi4d: A 4d egocentric dataset for category-level human-object interaction. In: Proceedings of the IEEE/CVF Conference on Computer Vision and Pattern Recognition. pp. 21013–21022 (2022)
39. Lockman, J.J., Kahrs, B.A.: New insights into the development of human tool use. *Current directions in psychological science* **26**(4), 330–334 (2017)
40. Long, X., Guo, Y.C., Lin, C., Liu, Y., Dou, Z., Liu, L., Ma, Y., Zhang, S.H., Habermann, M., Theobalt, C., et al.: Wonder3d: Single image to 3d using cross-domain diffusion. arXiv preprint arXiv:2310.15008 (2023)
41. Loper, M.M., Black, M.J.: Opendr: An approximate differentiable renderer. In: Computer Vision–ECCV 2014: 13th European Conference, Zurich, Switzerland, September 6–12, 2014, Proceedings, Part VII 13. pp. 154–169. Springer (2014)
42. Luma ai. capture 3d. <https://lumalabs.ai>. (2023)
43. Meng, H., Jin, S., Liu, W., Qian, C., Lin, M., Ouyang, W., Luo, P.: 3d interacting hand pose estimation by hand de-occlusion and removal. In: European Conference on Computer Vision. pp. 380–397. Springer (2022)
44. Mildenhall, B., Srinivasan, P.P., Tancik, M., Barron, J.T., Ramamoorthi, R., Ng, R.: Nerf: Representing scenes as neural radiance fields for view synthesis. *Communications of the ACM* **65**(1), 99–106 (2021)
45. Moon, G.: Bringing inputs to shared domains for 3d interacting hands recovery in the wild. In: Proceedings of the IEEE/CVF Conference on Computer Vision and Pattern Recognition. pp. 17028–17037 (2023)
46. Müller, T., Evans, A., Schied, C., Keller, A.: Instant neural graphics primitives with a multiresolution hash encoding. *ACM Transactions on Graphics (ToG)* **41**(4), 1–15 (2022)
47. Mur-Artal, R., Montiel, J.M.M., Tardos, J.D.: Orb-slam: a versatile and accurate monocular slam system. *IEEE transactions on robotics* **31**(5), 1147–1163 (2015)
48. Openai. gpt-4v(ision) system card. (2023)
49. Park, J.J., Florence, P., Straub, J., Newcombe, R., Lovegrove, S.: Deepsdf: Learning continuous signed distance functions for shape representation. In: Proceedings of the IEEE/CVF conference on computer vision and pattern recognition. pp. 165–174 (2019)
50. Park, J., Oh, Y., Moon, G., Choi, H., Lee, K.M.: Handocnet: Occlusion-robust 3d hand mesh estimation network. In: Proceedings of the IEEE/CVF Conference on Computer Vision and Pattern Recognition. pp. 1496–1505 (2022)
51. Patel, A., Wang, A., Radosavovic, I., Malik, J.: Learning to imitate object interactions from internet videos. arXiv preprint arXiv:2211.13225 (2022)
52. Pavlakos, G., Shan, D., Radosavovic, I., Kanazawa, A., Fouhey, D., Malik, J.: Reconstructing hands in 3d with transformers. arXiv preprint arXiv:2312.05251 (2023)
53. Prakash, A., Chang, M., Jin, M., Gupta, S.: Learning hand-held object reconstruction from in-the-wild videos. arXiv preprint arXiv:2305.03036 (2023)
54. Qi, C.R., Su, H., Mo, K., Guibas, L.J.: Pointnet: Deep learning on point sets for 3d classification and segmentation. In: Proceedings of the IEEE conference on computer vision and pattern recognition. pp. 652–660 (2017)
55. Qi, C.R., Yi, L., Su, H., Guibas, L.J.: Pointnet++: Deep hierarchical feature learning on point sets in a metric space. *Advances in neural information processing systems* **30** (2017)
56. Qu, W., Cui, Z., Zhang, Y., Meng, C., Ma, C., Deng, X., Wang, H.: Novel-view synthesis and pose estimation for hand-object interaction from sparse views. In:

- Proceedings of the IEEE/CVF International Conference on Computer Vision. pp. 15100–15111 (2023)
57. Ranftl, R., Bochkovskiy, A., Koltun, V.: Vision transformers for dense prediction. ArXiv preprint (2021)
 58. Ravi, N., Reizenstein, J., Novotny, D., Gordon, T., Lo, W.Y., Johnson, J., Gkioxari, G.: Accelerating 3d deep learning with pytorch3d. arXiv preprint arXiv:2007.08501 (2020)
 59. Reizenstein, J., Shapovalov, R., Henzler, P., Sbordone, L., Labatut, P., Novotny, D.: Common objects in 3d: Large-scale learning and evaluation of real-life 3d category reconstruction. In: Proceedings of the IEEE/CVF International Conference on Computer Vision. pp. 10901–10911 (2021)
 60. Reizenstein, J., Shapovalov, R., Henzler, P., Sbordone, L., Labatut, P., Novotny, D.: Common objects in 3d: Large-scale learning and evaluation of real-life 3d category reconstruction. In: International Conference on Computer Vision (2021)
 61. Romero, J., Kjellström, H., Kragic, D.: Hands in action: real-time 3d reconstruction of hands in interaction with objects. In: ICRA (2010)
 62. Romero, J., Tzionas, D., Black, M.J.: Embodied hands: Modeling and capturing hands and bodies together. arXiv preprint arXiv:2201.02610 (2022)
 63. Rong, Y., Shiratori, T., Joo, H.: Frankmocap: Fast monocular 3d hand and body motion capture by regression and integration. arXiv:2008.08324 (2020)
 64. Sann, C., Streri, A.: Perception of object shape and texture in human newborns: evidence from cross-modal transfer tasks. *Developmental science* **10**(3), 399–410 (2007)
 65. Scharstein, D., Szeliski, R.: A taxonomy and evaluation of dense two-frame stereo correspondence algorithms. *International journal of computer vision* **47**, 7–42 (2002)
 66. Shan, D., Geng, J., Shu, M., Fouhey, D.F.: Understanding human hands in contact at internet scale. In: Proceedings of the IEEE/CVF conference on computer vision and pattern recognition. pp. 9869–9878 (2020)
 67. Squeri, V., Sciutti, A., Gori, M., Masia, L., Sandini, G., Konczak, J.: Two hands, one perception: how bimanual haptic information is combined by the brain. *Journal of Neurophysiology* **107**(2), 544–550 (2012)
 68. Szeliski, R.: *Computer vision: algorithms and applications*. Springer Nature (2022)
 69. Taketomi, T., Uchiyama, H., Ikeda, S.: Visual slam algorithms: A survey from 2010 to 2016. *IPSJ Transactions on Computer Vision and Applications* **9**(1), 1–11 (2017)
 70. Tekin, B., Bogo, F., Pollefeys, M.: H+ o: Unified egocentric recognition of 3d hand-object poses and interactions. In: Proceedings of the IEEE/CVF conference on computer vision and pattern recognition. pp. 4511–4520 (2019)
 71. Tewari, A., Fried, O., Thies, J., Sitzmann, V., Lombardi, S., Sunkavalli, K., Martin-Brualla, R., Simon, T., Saragih, J., Nießner, M., et al.: State of the art on neural rendering. In: *Computer Graphics Forum*. vol. 39, pp. 701–727. Wiley Online Library (2020)
 72. Tomasi, C., Kanade, T.: Shape and motion from image streams under orthography: a factorization method. *International journal of computer vision* **9**, 137–154 (1992)
 73. Tse, T.H.E., Kim, K.I., Leonardis, A., Chang, H.J.: Collaborative learning for hand and object reconstruction with attention-guided graph convolution. In: Proceedings of the IEEE/CVF Conference on Computer Vision and Pattern Recognition. pp. 1664–1674 (2022)

74. Tzionas, D., Ballan, L., Srikantha, A., Aponte, P., Pollefeys, M., Gall, J.: Capturing hands in action using discriminative salient points and physics simulation. *International Journal of Computer Vision* **118**, 172–193 (2016)
75. Vaswani, A., Shazeer, N., Parmar, N., Uszkoreit, J., Jones, L., Gomez, A.N., Kaiser, Ł., Polosukhin, I.: Attention is all you need. *Advances in neural information processing systems* **30** (2017)
76. Wang, C., Zhu, F., Wen, S.: Memahand: Exploiting mesh-mano interaction for single image two-hand reconstruction. In: *Proceedings of the IEEE/CVF Conference on Computer Vision and Pattern Recognition*. pp. 564–573 (2023)
77. Wang, C., Zhu, F., Wen, S.: Memahand: Exploiting mesh-mano interaction for single image two-hand reconstruction. In: *Proceedings of the IEEE/CVF Conference on Computer Vision and Pattern Recognition (CVPR)*. pp. 564–573 (June 2023)
78. Wang, D., Cui, X., Chen, X., Zou, Z., Shi, T., Salcudean, S., Wang, Z.J., Ward, R.: Multi-view 3d reconstruction with transformers. In: *Proceedings of the IEEE/CVF International Conference on Computer Vision*. pp. 5722–5731 (2021)
79. Wang, P., Liu, L., Liu, Y., Theobalt, C., Komura, T., Wang, W.: Neus: Learning neural implicit surfaces by volume rendering for multi-view reconstruction. *arXiv preprint arXiv:2106.10689* (2021)
80. Wen, B., Tremblay, J., Blukis, V., Tyree, S., Müller, T., Evans, A., Fox, D., Kautz, J., Birchfield, S.: Bundlesdf: Neural 6-dof tracking and 3d reconstruction of unknown objects. In: *Proceedings of the IEEE/CVF Conference on Computer Vision and Pattern Recognition*. pp. 606–617 (2023)
81. Wen, C., Zhang, Y., Li, Z., Fu, Y.: Pixel2mesh++: Multi-view 3d mesh generation via deformation. In: *Proceedings of the IEEE/CVF international conference on computer vision*. pp. 1042–1051 (2019)
82. Wen, Y., Pan, H., Yang, L., Pan, J., Komura, T., Wang, W.: Hierarchical temporal transformer for 3d hand pose estimation and action recognition from egocentric rgb videos. In: *Proceedings of the IEEE/CVF Conference on Computer Vision and Pattern Recognition (CVPR)*. pp. 21243–21253 (June 2023)
83. Wilson, F.R.: *The hand: How its use shapes the brain, language, and human culture*. Vintage (1999)
84. Worchel, M., Diaz, R., Hu, W., Schreer, O., Feldmann, I., Eisert, P.: Multi-view mesh reconstruction with neural deferred shading. In: *Proceedings of the IEEE/CVF Conference on Computer Vision and Pattern Recognition*. pp. 6187–6197 (2022)
85. Wu, C.Y., Johnson, J., Malik, J., Feichtenhofer, C., Gkioxari, G.: Multiview compressive coding for 3d reconstruction. In: *Proceedings of the IEEE/CVF Conference on Computer Vision and Pattern Recognition*. pp. 9065–9075 (2023)
86. Xie, H., Yao, H., Sun, X., Zhou, S., Zhang, S.: Pix2vox: Context-aware 3d reconstruction from single and multi-view images. In: *Proceedings of the IEEE/CVF international conference on computer vision*. pp. 2690–2698 (2019)
87. Xie, X., Bhatnagar, B.L., Pons-Moll, G.: Chore: Contact, human and object reconstruction from a single rgb image. In: *European Conference on Computer Vision*. pp. 125–145. Springer (2022)
88. Xu, H., Wang, T., Tang, X., Fu, C.W.: H2onet: Hand-occlusion-and-orientation-aware network for real-time 3d hand mesh reconstruction. In: *Proceedings of the IEEE/CVF Conference on Computer Vision and Pattern Recognition (CVPR)*. pp. 17048–17058 (June 2023)
89. Yang, L., Li, K., Zhan, X., Lv, J., Xu, W., Li, J., Lu, C.: Artiboost: Boosting articulated 3d hand-object pose estimation via online exploration and synthesis.

- In: Proceedings of the IEEE/CVF Conference on Computer Vision and Pattern Recognition. pp. 2750–2760 (2022)
90. Ye, Y., Gupta, A., Tulsiani, S.: What’s in your hands? 3d reconstruction of generic objects in hands. In: Proceedings of the IEEE/CVF Conference on Computer Vision and Pattern Recognition. pp. 3895–3905 (2022)
 91. Ye, Y., Hebbar, P., Gupta, A., Tulsiani, S.: Diffusion-guided reconstruction of everyday hand-object interaction clips. In: Proceedings of the IEEE/CVF International Conference on Computer Vision. pp. 19717–19728 (2023)
 92. Yonas, A., Granrud, C.E.: The development of sensitivity of kinetic, binocular and pictorial depth information in human infants. In: Brain mechanisms and spatial vision, pp. 113–145. Springer (1985)
 93. Yu, Z., Huang, S., Fang, C., Breckon, T.P., Wang, J.: Acr: Attention collaboration-based regressor for arbitrary two-hand reconstruction. In: Proceedings of the IEEE/CVF Conference on Computer Vision and Pattern Recognition. pp. 12955–12964 (2023)
 94. Yu, Z., Huang, S., Fang, C., Breckon, T.P., Wang, J.: Acr: Attention collaboration-based regressor for arbitrary two-hand reconstruction. In: Proceedings of the IEEE/CVF Conference on Computer Vision and Pattern Recognition (CVPR). pp. 12955–12964 (June 2023)
 95. Zhang, C., Jiao, G., Di, Y., Huang, Z., Wang, G., Zhang, R., Fu, B., Tombari, F., Ji, X.: Moho: Learning single-view hand-held object reconstruction with multi-view occlusion-aware supervision. arXiv preprint arXiv:2310.11696 (2023)
 96. Zuo, B., Zhao, Z., Sun, W., Xie, W., Xue, Z., Wang, Y.: Reconstructing interacting hands with interaction prior from monocular images. In: Proceedings of the IEEE/CVF International Conference on Computer Vision. pp. 9054–9064 (2023)